View metadata, citation and similar papers at core.ac.uk
brought to you by CORE
provided by ScholarWorks@UNIST

AIP Applied Physics Letters

Doping-tunable thermal emission from plasmon polaritons in semiconductor epsilon-near-zero thin films

Young Chul Jun, Ting S. Luk, A. Robert Ellis, John F. Klem, and Igal Brener

Citation: Applied Physics Letters **105**, 131109 (2014); doi: 10.1063/1.4896573
View online: http://dx.doi.org/10.1063/1.4896573
View Table of Contents: http://scitation.aip.org/content/aip/journal/apl/105/13?ver=pdfcov
Published by the AIP Publishing

Articles you may be interested in

Ultrafast plasmonics using transparent conductive oxide hybrids in the epsilon-near-zero regime
Appl. Phys. Lett. **102**, 121112 (2013); 10.1063/1.4798833

N-type conductivity and properties of carbon-doped InN(0001) films grown by molecular beam epitaxy
J. Appl. Phys. **113**, 033501 (2013); 10.1063/1.4775736

Thermal and optical characterization of resonant coupling between surface plasmon polariton and semiconductor waveguides
Appl. Phys. Lett. **99**, 181118 (2011); 10.1063/1.3658733

Tamm plasmon polaritons: Slow and spatially compact light
Appl. Phys. Lett. **92**, 251112 (2008); 10.1063/1.2952486

Terahertz emission mediated by surface plasmon polaritons in doped semiconductors with surface grating
J. Appl. Phys. **103**, 056101 (2008); 10.1063/1.2840063

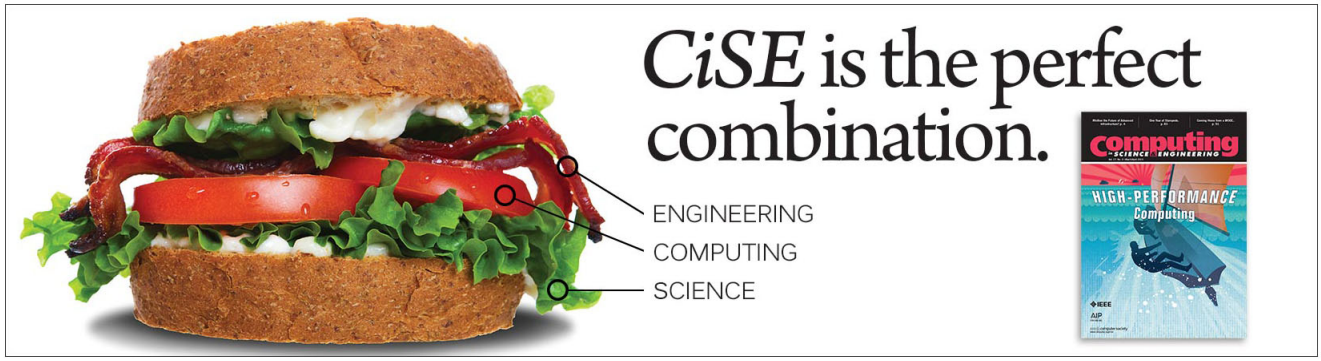

This article is copyrighted as indicated in the article. Reuse of AIP content is subject to the terms at: http://scitation.aip.org/termsconditions. Downloaded to IP: 114.70.4.138
On: Wed, 09 Sep 2015 01:19:07

Doping-tunable thermal emission from plasmon polaritons in semiconductor epsilon-near-zero thin films

Young Chul Jun,[1,a)] Ting S. Luk,[2,3,b)] A. Robert Ellis,[3] John F. Klem,[3] and Igal Brener[2,3]
[1]*Department of Physics, Inha University, Incheon 402-751, South Korea*
[2]*Center for Integrated Nanotechnologies, Sandia National Laboratories, Albuquerque, New Mexico 87185, USA*
[3]*Sandia National Laboratories, Albuquerque, New Mexico 87185, USA*

(Received 10 September 2014; accepted 14 September 2014; published online 30 September 2014)

We utilize the unique dispersion properties of leaky plasmon polaritons in epsilon-near-zero (ENZ) thin films to demonstrate thermal radiation control. Owing to its highly flat dispersion above the light line, a thermally excited leaky wave at the ENZ frequency out-couples into free space without any scattering structures, resulting in a narrowband, wide-angle, p-polarized thermal emission spectrum. We demonstrate this idea by measuring angle- and polarization-resolved thermal emission spectra from a single layer of unpatterned, doped semiconductors with deep-subwavelength film thickness ($d/\lambda_0 \sim 6 \times 10^{-3}$, where d is the film thickness and λ_0 is the free space wavelength). We show that this semiconductor ENZ film effectively works as a leaky wave thermal radiation antenna, which generates far-field radiation from a thermally excited mode. The use of semiconductors makes the radiation frequency highly tunable by controlling doping densities and also facilitates device integration with other components. Therefore, this leaky plasmon polariton emission from semiconductor ENZ films provides an avenue for on-chip control of thermal radiation.
© *2014 AIP Publishing LLC*. [http://dx.doi.org/10.1063/1.4896573]

Control of thermal radiation has been intensively studied for important energy conversion applications such as thermophotovoltaics and infrared (IR) sources. Surface gratings or resonant structures have been adopted to alter thermal radiation properties and achieve spectrally selective thermal emission.[1–14] In such patterns, narrowband thermal emission could be obtained at desired frequencies, which are determined by the pattern geometry. In addition, it is possible to get directional thermal emission by adjusting the scattering properties of structured surfaces.[3,11] Especially, surface waves are useful for engineering the properties of thermal radiation. Surface phonon polaritons on SiC and surface plasmon polaritons on metals or doped semiconductors have been used to tailor angular and spectral properties of thermal emission. However, these surface waves still need scatterers or antenna structures to convert them to far-field radiation.

Recently, there have been interesting studies on transverse-magnetic (TM) waveguide modes near the epsilon zero frequency of a material.[15–18] Ultra-thin materials can support both leaky and bound modes around the epsilon-near-zero (ENZ) frequency with highly flat dispersion. The leaky waves in ENZ films correspond to what has been called Berreman absorption[19] and can naturally out-couple into free space without any surface patterning. Here, we utilize the unique optical properties of these leaky waves in ENZ films and demonstrate spectrally selective thermal emission. Unlike previous studies on structured surfaces, we employ an unpatterned, doped semiconductor layer with a deep-subwavelength film thickness ($d \ll \lambda_0$, where d is the film thickness and λ_0 is the free space wavelength). These doped semiconductor thin films support leaky plasmon polariton modes at the ENZ frequency, which can be thermally excited and out-coupled to the far field without any scattering structures. This leaky plasmon polaritons emission manifests its highly flat dispersion characteristics; it produces a narrowband, wide-angle, p-polarized thermal emission spectrum. We experimentally verify this idea through the direct measurement of angle- and polarization-resolved thermal emission spectra.

There have been several studies on thermal emission control from planar structures in the past.[20–22] But those studies employed a complicated multilayer stack to form Fabry-Perot resonators or one-dimensional photonic crystals. Recently, there was also a theoretical study on thermal emission from ENZ metamaterials consisting of metal-dielectric multi-layer stacks or metal nanowire arrays.[23] In contrast, in our work, we use a single layer of ultra-thin, doped semiconductor and clarify the role of leaky modes existing in such ENZ thin films. The use of semiconductors makes the thermal radiation frequency (i.e., ENZ frequency) easily tunable during the material growth by controlling doping densities. It also facilitates device integration with other chip components. Therefore, leaky modes of semiconductor ENZ films can be a useful tool for on-chip control of thermal radiation.

Figure 1(a) shows a schematic of the sample structure studied here. A doped semiconductor thin film is grown on an undoped substrate, and the sample is heated on a hot plate. The leaky plasmon polariton mode in the doped semiconductor layer is thermally excited and out-couples to the far field, generating a narrowband thermal emission spectrum from an unpatterned film.

To understand the physical nature of this leaky mode, we first examine the dispersion properties of the different optical modes in doped-semiconductor ENZ thin films. The

[a)]youngchul.jun@inha.ac.kr,
[b)]tsluk@sandia.gov

 © 2014 AIP Publishing LLC

This article is copyrighted as indicated in the article. Reuse of AIP content is subject to the terms at: http://scitation.aip.org/termsconditions. Downloaded to IP: 114.70.4.138 On: Wed, 09 Sep 2015 01:19:07

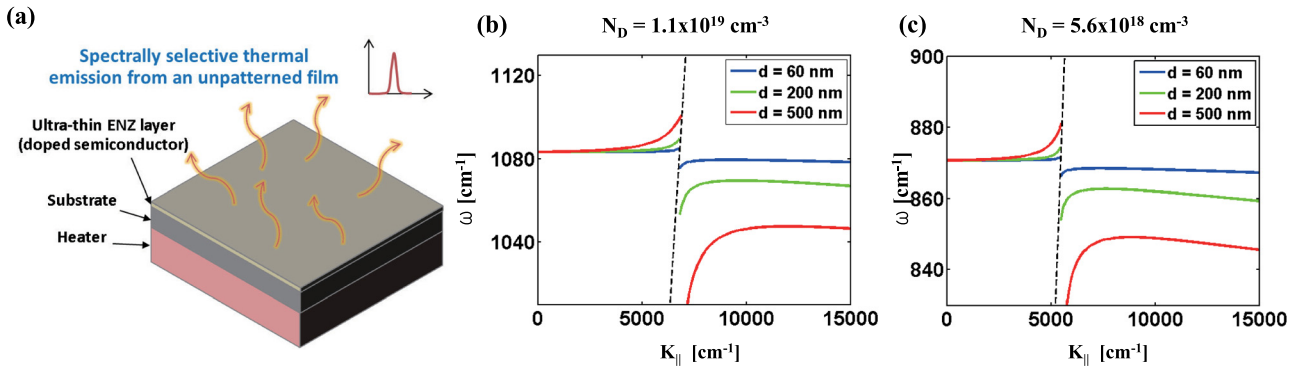

FIG. 1. (a) Schematic of leaky wave thermal emission. The sample including an ultra-thin doped semiconductor layer is heated using a hot plate. Thermally excited leaky modes are naturally out-coupled to far-field, generating a narrowband thermal emission spectrum at the ENZ frequency. (b) and (c) Dispersion relations of Berreman and ENZ modes for two different InAs doping densities: (b) $N_D = 1.1 \times 10^{19}\,cm^{-3}$, (c) $N_D = 5.6 \times 10^{18}\,cm^{-3}$. Dotted black lines are the light line in air.

dielectric constant ε of a semiconductor material can be modeled using the Drude approximation

$$\varepsilon = \varepsilon_\infty \left(1 - \frac{\omega_p^2}{\omega^2 + i\omega\Gamma}\right), \tag{1}$$

where $\omega_p = \sqrt{Nq^2/(\varepsilon_0 \varepsilon_\infty m^*)}$ is the plasma frequency, ε_∞ is the high frequency dielectric constant, ω is the angular frequency of incident light, N is the electron density, m^* is the electron effective mass, and Γ is the damping coefficient. In doped semiconductors, the frequency where the real part of the dielectric constant (Re[ε]) becomes zero can be controlled by adjusting the doping density (the doping density N affects the plasma frequency and, in turn, the dielectric constant ε). The dispersion relation for p-polarized modes in an asymmetric three-layer structure can be obtained by numerically solving the following relation:

$$\left(1 + \frac{\varepsilon_1 k_{z3}}{\varepsilon_3 k_{z1}}\right) = i\,\tan(k_{z2} d)\left(\frac{\varepsilon_2 k_{z3}}{\varepsilon_3 k_{z2}} + \frac{\varepsilon_1 k_{z2}}{\varepsilon_2 k_{z1}}\right), \tag{2}$$

where $k_{zn} = (\varepsilon_n \omega^2/c^2 - k_{||}^2)^{1/2}$. We calculated the dispersion relations for an [air/n+ InAs/substrate] structure for several ENZ layer (i.e., n+ InAs) thicknesses. We assumed undoped GaAs as our substrate and used the dielectric constants obtained by ellipsometry measurements. In Fig. 1(b), the doping density is $N_D = 1.1 \times 10^{19}\,cm^{-3}$ and the ENZ frequency is $\sim 1080\,cm^{-1}$ (the horizontal dashed line). In Fig. 1(c), the doping density is $N_D = 5.6 \times 10^{18}\,cm^{-3}$ and the ENZ frequency is reduced to $\sim 870\,cm^{-1}$. In both cases, the dispersion curves are divided into two branches; one is on the left side of the light line (i.e., leaky modes) and are called Berreman modes, and the other is on the right side of the light line (i.e., bound modes) and are called ENZ modes.[15] As the ENZ layer thickness d decreases, both modes approach the epsilon zero frequency (Re[ε] = 0), and the dispersion curves become highly flat. Because there is no mode cutoff as the film thickness is decreased, these modes can even exist in films with truly nanoscale thicknesses. The mode properties are mainly determined by the ENZ layer itself (i.e., doped semiconductor); similar Berreman and ENZ modes even exist on a metal substrate, and the mode dispersion relations do not change significantly.

ENZ modes are bound modes, and thus cannot couple to free space optical modes without a scattering or antenna structure. However, Berreman modes are leaky modes and will couple to free space even when excited thermally. Furthermore, for thin films, the Berreman mode dispersion becomes highly flat. Therefore, this leaky radiation should be spectrally narrow. At the same time, it should be strongly p-polarized because it originates from a p-polarized mode. We utilize these unique properties of Berreman modes to demonstrate p-polarized, narrowband, doping-tunable thermal radiation from unpatterned, ultra-thin semiconductor films.

We prepared two semiconductor wafers (wafers A and B) grown using molecular beam epitaxy (MBE). Undoped 100 nm GaAs and 1000 nm AlSb buffer epilayers were first grown on a semi-insulating GaAs substrate, followed by the growth of a 60 nm n+ InAs epilayer and a 30 nm undoped InAs cap layer. In wafer A, the doping density of n+ InAs ENZ layer was $N_D = 1.1 \times 10^{19}\,cm^{-3}$, and in wafer B, $N_D = 5.6 \times 10^{18}\,cm^{-3}$. These doping densities were determined by Hall measurements after wafer growth.

The wafers were first characterized by optical absorption measurements. Because Berreman modes can be excited by free-space coupling of light, the absorption spectrum should exhibit these spectral features. To verify this, we performed hemispherical directional reflectometer (HDR) measurements (Surface Optics SOC-100) with a broadband thermal IR source. The reflectivity and transmissivity spectra of the samples were measured at room temperature for different incident angles to obtain absorptivity ($A = 1 - R - T$). Figure 2 shows the measured absorption spectra from wafers A and B. These measurements were repeated by varying the incidence angle in 15° increments, and thus we obtained angle-resolved absorption spectra for p- and s-polarizations of the incident light. As we expected from the properties of Berreman modes, we have strong absorption peaks around the ENZ frequency in the p-polarized spectra. In wafer A ($N_D = 1.1 \times 10^{19}\,cm^{-3}$), strong absorption peaks appeared around $1080\,cm^{-1}$ in the p-polarized spectra at all angles (Fig. 2(a)). However, in the s-polarized spectra (Fig. 2(b)), there were only very weak features around the ENZ frequency. In wafer B ($N_D = 5.6 \times 10^{18}\,cm^{-3}$), the ENZ frequency is at a lower frequency (around $870\,cm^{-1}$) due to the

This article is copyrighted as indicated in the article. Reuse of AIP content is subject to the terms at: http://scitation.aip.org/termsconditions. Downloaded to IP: 114.70.4.138 On: Wed, 09 Sep 2015 01:19:07

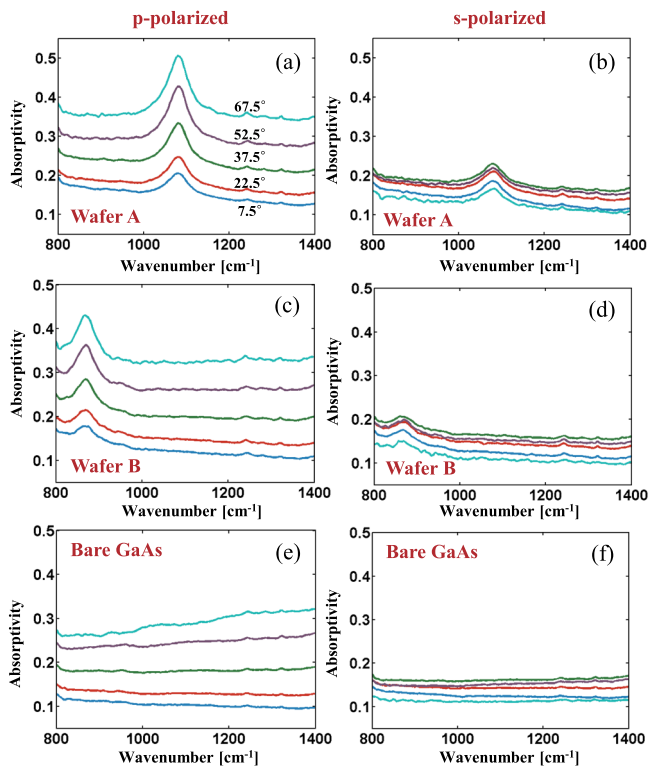

FIG. 2. Angle-resolved, polarization-dependent absorptivity measurements for p- and s-polarizations. (a) and (b) Wafer A (60 nm n+ InAs, $N_D = 1.1 \times 10^{19}\,cm^{-3}$): we have strong absorption peaks around the ENZ frequency in the p-polarized spectra. (c) and (d) Wafer B (60 nm n+ InAs, $N_D = 5.6 \times 10^{18}\,cm^{-3}$): the ENZ peak in the p-polarized spectrum moves to a lower frequency due to the reduced doping level. All these features manifest optical characteristics of Berreman modes in doped semiconductor thin films. (e) and (f) The absorption spectra of an undoped GaAs substrate are also shown for comparison.

reduced doping density. Again, the p-polarized spectra showed clear absorption peaks (Fig. 2(c)), while the s-polarized spectra had very weak features (Fig. 2(d)). These absorption features agree well with the dispersion properties that we discussed above. We also measured absorption spectra of a bare GaAs substrate for comparison, and there were no sharp features for both polarizations (Figs. 2(e) and 2(f)). We can easily understand this from the fact that Berreman modes do not exist in such undoped substrate.

According to Kirchhoff's law of thermal radiation, the absorptivity of an object should be equal to its emissivity ($A = \epsilon$) for each frequency and each incident angle at thermal equilibrium. Therefore, we expect to obtain narrow-band thermal emission spectra from these samples. Due to Kirchhoff's law, emissivity is often deduced from reflectivity and transmissivity measurements. However, standard reflectivity and transmissivity measurements often fail to detect scattered light from a sample. We avoid such inaccuracies by directly measuring thermal emission spectra as a function of angle. Furthermore, we also perform accurate background correction by placing a well-calibrated reference material together with the sample in a thermally uniform environment.[24,25] Figure 3 shows a schematic of the setup for our angle- and polarization-resolved thermal emission measurements. It consists of a vacuum chamber attached to a Fourier-transform infrared spectrometer

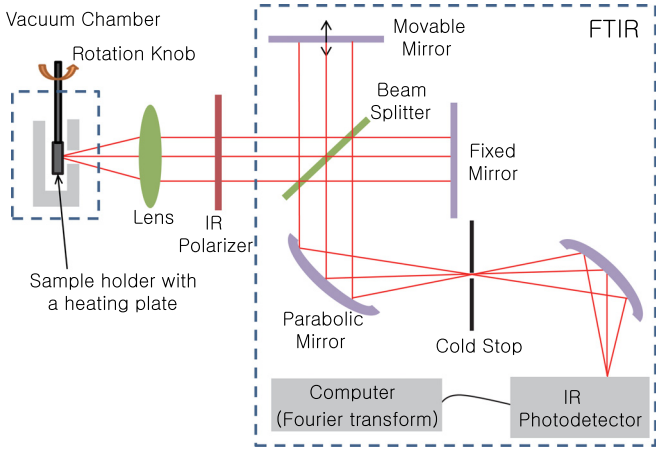

FIG. 3. Schematic of the setup for angle- and polarization-resolved thermal emission measurements.

(FTIR). We performed FTIR external source mode measurements. The sample and reference materials were heated to 140 °C using a hot plate inside the vacuum chamber, and thermal emission spectra were measured for different sample tilt angles. For each measurement, the polarization of the incident light was varied to be either p- or s-polarized.

Figure 4 shows the measured emissivity spectra from wafers A and B. For these emission spectra, thermal emission spectra exhibit a clear difference between p- and s-polarizations. Only p-polarized spectra show very sharp thermal emission peaks around the ENZ frequency. In wafer A, the emission peak appeared around 1050 cm^{-1} (Fig. 4(a)), superimposed on a feature-less background emission spectrum that corresponds to the bulk GaAs substrate. It is worth noticing that even though we have an ultra-thin, doped semiconductor layer, we observe a clear emission peak. Here, the film thickness (60 nm) corresponds to $d/\lambda_0 \sim 6 \times 10^{-3}$, where d is the film thickness and λ_0 is the free space wavelength. In wafer B, the peak again appears at a lower frequency (around 850 cm^{-1}) due to the reduced doping density (Fig. 4(c)). In both wafers, there are only much weaker features in the s-polarized emissivity spectra (Figs. 4(b) and 4(d)). As expected, there is a very clear contrast between the p- and s-polarization measurements. The peak positions are similar to those in the absorption spectra, but they are slightly red-shifted due to the elevated temperature for thermal measurements.[26] We also measured the thermal emissivity of a bare GaAs substrate. The bare substrate gives no features around the ENZ frequency for both p- and s-polarizations. Bulk GaAs emission could be eliminated by removing the carrier substrate and transferring the doped layer to a low-emissivity substrate. Or, the doped layer could be grown on a low-emissivity substrate from the beginning. An emissivity close to one can be also achieved if the undoped GaAs is replaced with metal (e.g., see the perfect absorption scheme in Ref. 27).

Our measurements clearly show that unpatterned semiconductor thin films generate spectrally selective thermal emission near the ENZ frequencies that are determined purely by doping densities. Thermally excited Berreman modes in the doped semiconductor radiate to free space due to the leaky nature of the Berreman modes. Thus, an

This article is copyrighted as indicated in the article. Reuse of AIP content is subject to the terms at: http://scitation.aip.org/termsconditions. Downloaded to IP: 114.70.4.138 On: Wed, 09 Sep 2015 01:19:07

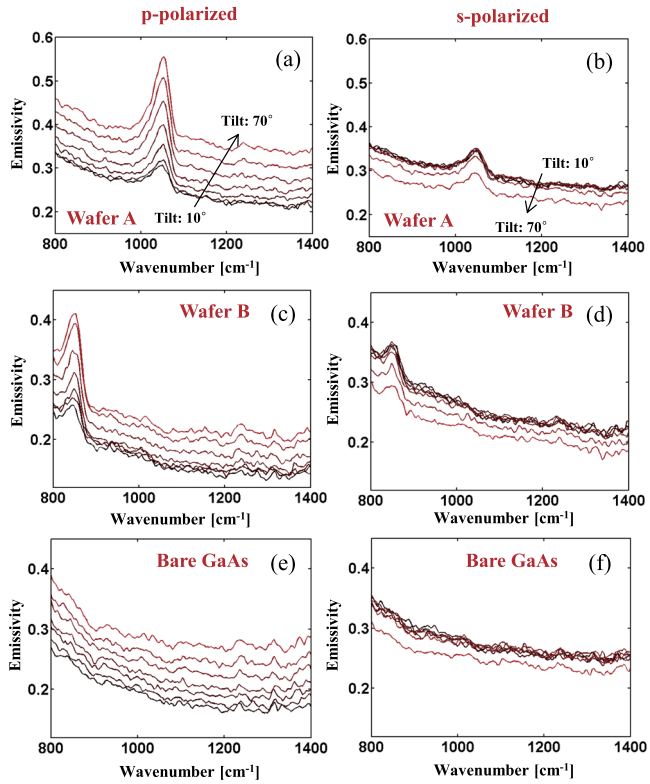

FIG. 4. Angle-resolved, polarization-dependent emissivity measurements for p- and s-polarizations at 140 °C. (a) and (b) Wafer A (60 nm n+ InAs, $N_D = 1.1 \times 10^{19}$ cm^{-3}): p-polarized spectra show very sharp thermal emission peaks around the ENZ frequency. (c) and (d) Wafer B (60 nm n+ InAs, $N_D = 5.6 \times 10^{18}$ cm^{-3}): the peaks appear at a lower frequency due to the reduced doping density. (e) and (f) Thermal emissivity spectra from an undoped GaAs substrate.

ultra-thin ENZ film effectively works as a leaky wave thermal antenna,[6,10] which converts a thermally excited mode to far-field radiation. Some of the early studies of Berreman modes were done under thermal excitation followed by emission measurements,[28] but they were limited to phonon-polariton Berreman modes, where the mode frequency is fixed by the optical phonons in the material. Here, we utilize plasmon polariton Berreman modes, where the emission can be tuned simply by changing the doping density. We used unpatterned, doped semiconductors with properties (material, doping level, thickness, etc.) that can be directly controlled during the growth process. Therefore, this can greatly simplify the device structure and fabrication for thermal radiation control. The use of semiconductors also facilitates device integration with other chip components. Therefore, the leaky wave thermal emission from doped semiconductor films can be a useful tool for on-chip control of thermal radiation, such as energy conversion and thermal management (chip cooling). A doped semiconductor layer can be also used as an electrical current channel, and it could be possible to heat a sample electrically without a bulky hot plate. This can be useful for implementing chip-scale thermal emitters at IR frequencies where efficient sources are less readily available.

Finally, we performed numerical calculations and compared them with the Berreman mode dispersion. For an [air/ENZ film (n+ InAs, $N_D = 1.1 \times 10^{19}$ cm^{-3})/undoped GaAs substrate] structure, we calculated reflectivity (R) and transmissivity (T) numerically (using the transfer matrix method) and obtained absorptivity ($A = 1 - R - T$). Following Kirchhoff's law, emissivity should be the same as absorptivity. Figures 5(a) and 5(c) show absorptivity colormaps for p-polarized light incident from the air side. Absorptivity is plotted as a function of frequency and incidence angle. In Fig. 5(a), the n+ InAs layer thickness is d = 60 nm, and for Fig. 5(c), d = 500 nm. Both show strong absorption near the ENZ frequency (~1080 cm^{-1}). The thicker ENZ film has larger absorptivity, but the absorption peak is also broadened in the frequency domain (Fig. 5(c)). Berreman mode dispersion curves are also drawn in dotted white lines. We can see that absorption maxima occur along the Berreman mode dispersion curve exactly in both cases. S-polarized light produces completely different absorption behavior; Figures 5(b) and 5(d) show absorptivity colormaps for s-polarization

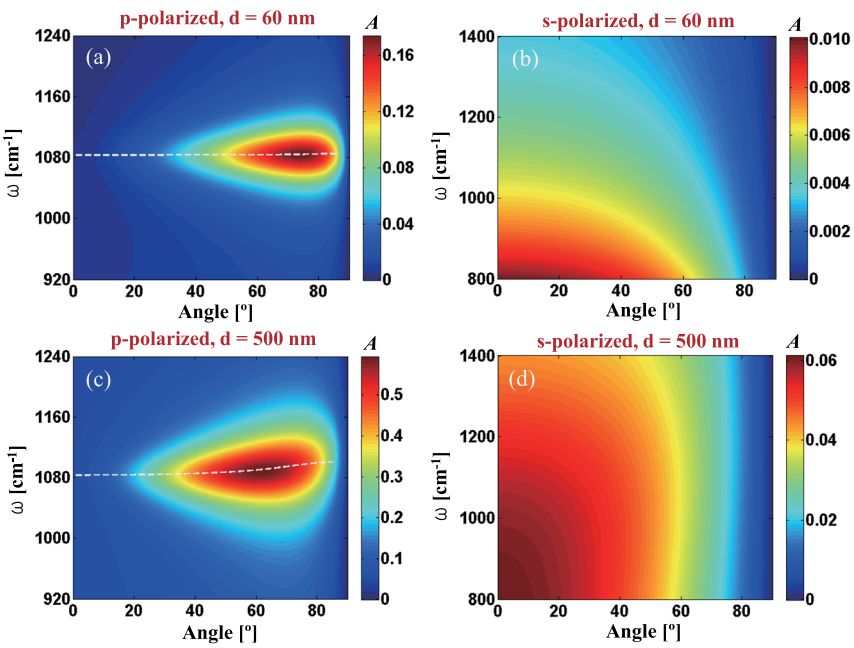

FIG. 5. Absorptivity calculation for an [air/ENZ/substrate] structure. (a) and (c) Strong absorption is observed near the ENZ frequency for p-polarized incident light. The Berreman mode dispersion relations are also shown in dotted white lines. In a thinner film (d = 60 nm), the Berreman mode dispersion is highly flat, while it is directed slightly upward in a thicker film (d = 500 nm). In both cases, absorption maxima occur along the Berreman mode dispersion curve. (b) and (d) Absorptivity calculation for s-polarization. Absorption is much weaker for s-polarization, and there are no narrowband features. Note that the color scale is different for each plot.

This article is copyrighted as indicated in the article. Reuse of AIP content is subject to the terms at: http://scitation.aip.org/termsconditions. Downloaded to IP: 114.70.4.138 On: Wed, 09 Sep 2015 01:19:07

(d = 60 nm for (b), d = 500 nm for (d)). Absorption is much weaker for s-polarization, and there are no narrowband features like those for p-polarization. These results agree well with our experiment results and confirm that our narrowband, p-polarized thermal emission originates from the leaky modes existing in ENZ thin films.

In summary, we utilized the unique optical properties of leaky plasmon polaritons modes in ENZ thin films and demonstrated spectrally selective thermal emission. We explained the thermal emission properties of doped semiconductor thin films in terms of the mode characteristics. Thermally excited leaky waves in unpatterned semiconductor films naturally outcouple into free space, and thus result in narrowband, wide-angle, p-polarized thermal emission spectra following the highly flat mode dispersion characteristics. We verified this idea through the direct measurements of angle-resolved and polarization-resolved thermal emission spectra. The unique properties of the leaky wave emission could lead to chip-scale, easy-to-fabricate thermal emitters operating throughout the entire IR frequency range.

This work was performed, in part, at the Center for Integrated Nanotechnologies, an Office of Science User Facility operated for the U.S. Department of Energy (DOE) Office of Science. Sandia National Laboratories is a multi-program laboratory managed and operated by Sandia Corporation, a wholly owned subsidiary of Lockheed Martin Corporation, for the U.S. Department of Energy's National Nuclear Security Administration under Contract DE-AC04-94AL85000. Parts of this work were supported by the U.S. Department of Energy, Office of Basic Energy Sciences, Division of Materials Sciences and Engineering. Y.C.J. acknowledges the supports from Inha University Research Grant (INHA-47839) and the National Research Foundation of Korea (NRF) grant funded by the Korea government (Ministry of Science, ICT and Future Planning; No. 2008-0061893).

[1]P. J. Hesketh, J. N. Zemel, and B. Gebhart, Nature **324**, 549–551 (1986).
[2]S.-Y. Lin, J. G. Fleming, E. Chow, J. Bur, K. K. Choi, and A. Goldberg, Phys. Rev. B **62**, R2243 (2000).
[3]J.-J. Greffet, R. Carminati, K. Joulain, J.-P. Mulet, S. Mainguy, and Y. Chen, Nature **416**, 61–64 (2002).
[4]H. Sai, Y. Kanamori, and H. Yugami, Appl. Phys. Lett. **82**, 1685 (2003).
[5]B. J. Lee, C. J. Fu, and Z. M. Zhang, Appl. Phys. Lett. **87**, 071904 (2005).
[6]M. Laroche, R. Carminati, and J.-J. Greffet, Phys. Rev. Lett. **96**, 123903 (2006).
[7]H. T. Miyazaki, K. Ikeda, T. Kasaya, K. Yamamoto, Y. Inoue, K. Fujimura, T. Kanakugi, M. Okada, K. Hatade, and S. Kitagawa, Appl. Phys. Lett. **92**, 141114 (2008).
[8]I. Puscasu and W. L. Schaich, Appl. Phys. Lett. **92**, 233102 (2008).
[9]N. Dahan, A. Niv, G. Biener, Y. Gorodetski, V. Kleiner, and E. Hasman, J. Heat Transfer **130**, 112401 (2008).
[10]J. A. Schuller, T. Taubner, and M. L. Brongersma, Nat. Photonics **3**, 658–661 (2009).
[11]S. E. Han and D. J. Norris, Opt. Express **18**, 4829–4837 (2010).
[12]X. Liu, T. Tyler, T. Starr, A. F. Starr, N. M. Jokerst, and W. J. Padilla, Phys. Rev. Lett. **107**, 045901 (2011).
[13]J. A. Mason, S. Smith, and D. Wasserman, Appl. Phys. Lett. **98**, 241105 (2011).
[14]V. Rinnerbauer, Y. X. Yeng, W. R. Chan, J. J. Senkevich, J. D. Joannopoulos, M. Soljacic, and I. Celanovic, Opt. Express **21**, 11482–11491 (2013).
[15]S. Vassant, J.-P. Hugonin, F. Marquier, and J.-J. Greffet, Opt. Express **20**, 23971–23977 (2012).
[16]S. Vassant, A. Archambault, F. Marquier, F. Pardo, U. Gennser, A. Cavanna, J. L. Pelouard, and J.-J. Greffet, Phys. Rev. Lett. **109**, 237401 (2012).
[17]S. Vassant, I. Moldovan Doyen, F. Marquier, F. Pardo, U. Gennser, A. Cavanna, J. L. Pelouard, and J. J. Greffet, Appl. Phys. Lett. **102**, 081125 (2013).
[18]Y. C. Jun, J. Reno, T. Ribaudo, E. Shaner, J.-J. Greffet, S. Vassant, F. Marquier, M. Sinclair, and I. Brener, Nano Lett. **13**, 5391 (2013).
[19]D. W. Berreman, Phys. Rev. **130**, 2193–2198 (1963).
[20]A. Narayanaswamy and G. Chen, Phys. Rev. B **70**, 125101 (2004).
[21]B. J. Lee and Z. M. Zhang, J. Appl. Phys. **100**, 063529 (2006).
[22]I. Celanovic, D. Perreault, and J. Kassakian, Phys. Rev. B **72**, 075127 (2005).
[23]S. Molesky, C. J. Dewalt, and Z. Jacob, Opt. Express **21**, A96–A110 (2012).
[24]A. R. Ellis, H. M. Graham, M. B. Sinclair, and J. C. Verley, Proc. SPIE **7065**, 706508 (2008).
[25]T. S. Luk, T. McLellan, G. Subramania, J. C. Verley, and I. El-Kady, Photonics Nanostruct. Fundam. Appl. **6**, 81–86 (2008).
[26]E. A. Shaner, J. G. Cederberg, and D. Wasserman, Appl. Phys. Lett. **91**, 181110 (2007).
[27]T. S. Luk, S. Campione, I. Kim, S. Feng, Y. C. Jun, S. Liu, J. B. Wright, I. Brener, P. B. Catrysse, S. Fan, and M. B. Sinclair, Phys. Rev. B **90**, 085411 (2014).
[28]K. Hisano, J. Phys. Soc. Jpn. **25**, 1091–1099 (1968).

This article is copyrighted as indicated in the article. Reuse of AIP content is subject to the terms at: http://scitation.aip.org/termsconditions. Downloaded to IP: 114.70.4.138 On: Wed, 09 Sep 2015 01:19:07